RASĀYAN *J. Chem.*
Vol. 19 | No. 1 | 483-491 | January-March | 2026
ISSN: 0974-1496 | e-ISSN: 0976-0083 | CODEN: RJCABP
http://www.rasayanjournal.com
http://www.rasayanjournal.co.in

ENHANCED METHYLENE BLUE ADSORPTIVE REMOVAL BY GREEN-SYNTHESIZED *Litchi chinensis*-SEED COPPER NANOPARTICLES UPON RSM OPTIMIZATION: KINETIC AND ISOTHERM PERSPECTIVES

Pampana Anil Kumar[1], Alpitha Suhasini Juttuka[2], M. Sudheera[3], Pulipati King[1], D. Appala Naidu[1], and Meena Vangalapati[1,✉]

[1]Dept. of Chemical Engineering, AU, Visakhapatnam-530003, AP, India.
[2]Dept. of Chemical and Petroleum Engineering, JNTUK, Kakinada-533003, AP, India.
[3]Dept. of Pharmaceutical Engineering, BVRIT, Narasapur, TG, India.
✉Corresponding author: meenasekhar2002@yahoo.com

ABSTRACT

Green-synthesised copper nanoparticles were made using an extract from *Litchi chinensis* seeds and were studied as an environmentally friendly material for eliminating methylene blue (MB) dye from an aqueous medium. The structural and morphological characteristics of the CuNPs were confirmed through FTIR, EDX, BET, and SEM analyses, demonstrating successful nanoparticle formation with functional groups capable of interacting with dye molecules. Using a CCD–RSM framework, the key operational parameters - pH, adsorbent dosage, contact time, and temperature - were systematically optimised, yielding a maximum MB removal efficiency of 88.5% under the optimal conditions (pH ≈ 8, 0.5 g/L, 30 min, and 318 K). The reliability of the predicted responses was confirmed by the statistical model's excellent fit (R^2 = 0.999). Kinetic results confirmed a pseudo-second-order mechanism, while equilibrium data revealed monolayer chemisorption according to the Langmuir isotherm. The thermodynamic assessment further affirmed the spontaneous and endothermic nature of the adsorption. Concurrently, CuNPs synthesised from litchi seeds offer a resource-efficient, environmentally compliant, and effective platform for treating dye-contaminated wastewater.

Keywords: Methylene Blue, Adsorption, CCD, RSM, CuNPs, Litchi Seed Extract, and Green Synthesis.

RASĀYAN *J. Chem.*, Vol. 19, No.1, 2026

INTRODUCTION

Many textile, leather, and paper industries release methylene blue (MB), a toxic, persistent, and possibly mutagenic dye that poses serious risks to human health and aquatic ecosystems.[1,2] Traditional methods like advanced oxidation, activated carbon adsorption, and coagulation are constrained by their expense, intricacy, and production of secondary waste.[3-5] A viable substitute is provided by nanotechnology, where copper nanoparticles (CuNPs) are preferred over noble metals due to their high surface area, adaptability, adjustable characteristics, activity of the catalyst, and affordability.[4-6] However, traditional CuNPs synthesis uses risky and energy-intensive techniques, which raises environmental issues. Recent studies using biogenic nanoparticles from various plant sources, showing their effectiveness and environmental friendliness in dye remediation, demonstrate that green synthesis using plant extracts offers a sustainable solution.[7–9] Using plant extracts for green synthesis provides an environmentally friendly method of producing nanoparticles, with sugars, flavonoids, and polyphenols serving as natural reducing agents.[10, 11] *Litchi chinensis* seeds, an abundant agro-waste material, contain high levels of phenolics, tannins, and amino acids, making them a sustainable and effective natural precursor for the green synthesis of copper nanoparticles.[12-14] These CuNPs made from *litchi chinensis* seed extract for the removal of methylene blue have not yet been investigated, despite lychee seed biochar having been investigated for dye adsorption.[15] This study presents a new, valuable method for using fruit waste, providing an economical and environmentally friendly wastewater treatment solution, and also supports SDG-6, i.e., clean water and sanitation by developing a green and efficient nanoparticle-based approach for improving wastewater quality through the effective removal of methylene blue.

http://doi.org/10.31788/RJC.2026.1919585

EXPERIMENTAL

Sustainable Production and Processing of Copper Nanoparticles from *Litchi chinensis* Seeds

Seeds of litchi (*Litchi chinensis*) were ground, dried, and extracted (100 g in 500 mL water at 80°C, 1 h). 0.005 M $CuSO_4 \cdot 2H_2O$ was mixed (1:1) with the filtrate, which acted as a stabilising and reducing agent. CuNPs formation was verified by a colour shift from light to dark brown. The product was cleaned, dried (373K, 12h), ground, centrifuged (4250 rpm, 30 min), and stored for characterisation and adsorption investigations.

Comprehensive Characterisation of Green-Synthesised CuNPs

The stability and successful formation of *litchi chinensis* seed-mediated CuNPs were validated by multiple analyses. While UV-Vis showed a clear SPR peak confirming nanoparticle synthesis, FTIR identified the phytochemicals in charge of reduction and capping. Copper was identified by EDX as the main element with trace amounts of bio-organic residues. Nanoscale, crystalline particles with a distinct morphology and regulated aggregation were visible in SEM. The CuNPs were generally well-stabilised and ideal for environmental remediation and dye adsorption.

Studies on Batch Adsorption

The MB adsorption studies were carried out in 250 mL Erlenmeyer flasks, each loaded with 50 mL of the dye solution (20 -100 mg/L), employing CuNPs dosages progressively increased from 0.1 to 1.0 g/L to assess removal efficiency. Temperatures (303–318 K), contact times (0–50 min), and pH (3–11) were all varied while the solutions were shaken (150 rpm). 0.1 M HCl/NaOH was used to adjust the pH. The remaining dye was measured using UV-Vis at 664 nm following centrifugation (5000 rpm, 10 min). % removal efficiency (R) and the capacity of adsorption (q_t and q_e (mg/g))[12-15] were computed using standard equations (1 and 2) based on C_0, C_t, C_e (mg/L), m (in g), V (in L).

$$q_t = \frac{(C_o - C_t)V}{m} \quad \text{and} \quad q_e = \frac{(C_o - C_e)V}{m} \qquad (1)$$

$$R(\%) = \frac{(C_o - C_e)}{C_o} \times 100 \qquad (2)$$

Thorough Isothermal, Kinetic, and Thermodynamic Analysis of Adsorption of MB Dye

The adsorption mechanism and process feasibility were elucidated by applying the Langmuir and the Freundlich isotherm frameworks to the experimental data, determining the thermodynamic parameters (ΔG°, ΔH°, and ΔS°), and analysing the kinetic behaviour through pseudo-first-order (PFO) and pseudo-second-order (PSO) models.

Isotherms of Adsorption

The equilibrium interaction between MB and CuNPs was evaluated using the Freundlich and Langmuir models. The Eq.-3 assumes monolayer adsorption on uniform sites as determined by q_{max} (mg/g) and K_L (L/mg). The heterogeneous multilayer adsorption process is described by Eq.-4, where n represents adsorption intensity and K_f ((mg/g) (L/mg)$^{1/n}$) indicates capacity. Therefore, the surface characteristics and binding mechanisms were revealed by model fitting.[10-12]

The Langmuir model is symbolised by the equation (3):

$$q_e = \frac{q_{max} K_L C_e}{1 + K_L C_e} \qquad (3)$$

The Freundlich model, depicted by equation (4):

$$q_e = K_f C_e^{1/n} \qquad (4)$$

Adsorption Kinetics

The kinetic behaviour was interpreted by applying both the PFO (Eq.-5) and PSO (Eq.-6) models to elucidate the kinetics governing the rate of MB uptake by the adsorbent. PFO assumes that the adsorption rate, which is determined by k_1 (min^{-1}), is proportional to vacant sites, whereas PSO ascribes MB uptake to valence-force-based chemisorption with a rate constant of k_2 (g/mg.min). By using comparative fitting

(R^2 and error analysis), the dominant kinetic pathway governing MB adsorption on CuNPs was identified.[13-15]

$$\ln(q_e - q_t) = \ln q_e - k_1 t \quad (5)$$

$$\frac{t}{q_t} = \frac{1}{k_2 q_e^{\,2}} + \frac{t}{q_e} \quad (6)$$

Studies of Thermodynamics

In order to investigate the feasibility and energy changes, MB adsorption onto green-synthesised CuNPs was assessed at various temperatures. The spontaneity and underlying thermodynamic characteristics of the adsorption system were elucidated by evaluating Kc at varying temperatures and applying the Van't Hoff model (Eq.-7) to derive ΔG°, ΔH°, and ΔS°.[13-15]

$$\Delta G^o = -RT \ln K_c$$

$$\ln K_c = \frac{\Delta S^o}{R} - \frac{\Delta H^o}{RT} \quad (7)$$

In this expression, T represents the absolute temperature measured in Kelvin, and R is the universal gas constant, which has a value of 8.314 Joules per mole per Kelvin.

The Assessment/Characterisation of Green-Synthesised Copper Nanoparticles

SEM analysis of green-synthesised CuNPs showed that they were widely distributed, primarily spherical, and exhibited little aggregation shown in Fig.-1a and 1b. Copper was identified by EDX as the predominant element with trace amounts of phytochemical residues, indicating stabilisation and capping depicted in Fig.-1c. With peak shifts following MB adsorption suggesting strong dye–surface interactions, FTIR spectra revealed –OH, C=O, and –NH groups involved in nanoparticle formation and stabilisation (Fig.-1d, and 1e). The BET analysis, performed using nitrogen adsorption at 77.350K, revealed a specific surface area of 3.688 m²/g, a pore volume of 0.011 cm^3/g, and a mesoporous average pore diameter of 2.248nm, indicating a low-surface-area material with small mesopores that can nonetheless facilitate effective adsorption through surface–chemical interactions. All of these findings support the effective synthesis of stable, functionalized CuNPs with advantageous surface characteristics for dye remediation.

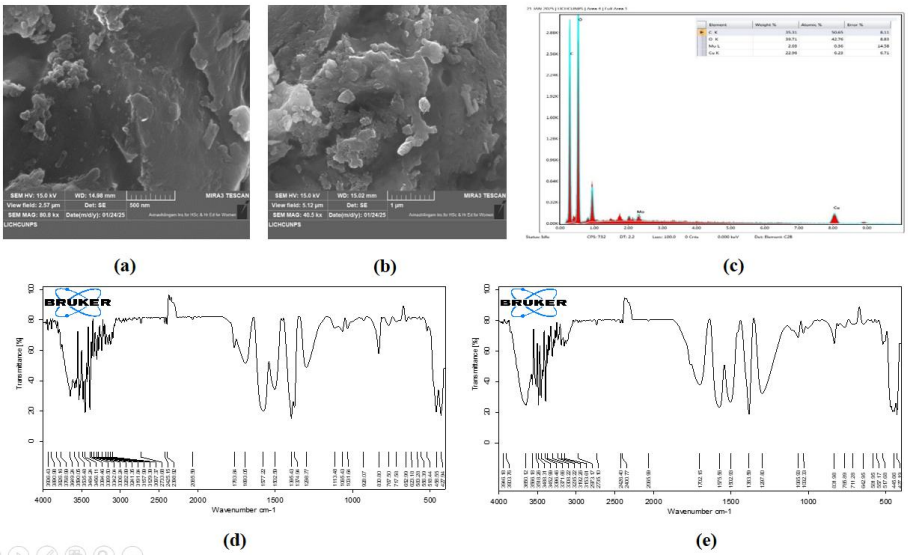

Fig.-1: (a and b). SEM Micrograph Showing the Green-Synthesised CuNPs Surface Morphology; (c). EDX Pattern of Green Synthesised CuNPs; (d and e). FTIR Spectra Showing the Shifts of the -OH, C=O, and -NH Groups Before and after MB Adsorption onto CuNPs.

Optimisation Using Response Surface Methodology (RSM)

Assessing variable interactions beyond single-factor experiments is necessary for effective dye removal.[8,13] Strong multivariate optimisation with fewer trials and better predictive accuracy is provided

by RSM, especially Central Composite Design (CCD). In the present investigation, a CCD–RSM framework implemented in Design-Expert v13 was employed to refine the operating conditions for MB adsorption onto CuNPs synthesised from litchi seeds. The optimisation considered four major factors, such as temperature (308–328 K), initial dye concentration (10–30 mg/L), adsorbent dose (0.3–0.7 g/L), and pH (6–10), with the experimental design matrix provided in Table-1. Removal efficiency (%) was modelled by a quadratic polynomial (Eq. 8), enabling identification of key factors and optimal conditions for sustainable wastewater treatment.

$$Y = \beta_0 + \sum \beta_i X_i + \sum \beta_{ii} X_i^2 + \sum \beta_{ij} X_i X_j \qquad (8)$$

Where: Y is the predicted removal efficiency, X_i are coded factors, and β values represent regression coefficients.

Table-1: Central Composite Design (CCD) Factors and Levels for RSM Optimisation.

Name of the Factor	Lowest value	Highest value	Coded low	Coded High
A: Concentration, mg/L	10.0	30.0	-1 ↔ 15.0	+1 ↔ 20.0
B: NP dosage g/L	0.3	0.7	-1 ↔ 0.4	+1 ↔ 0.6
C: pH	6.0	10.0	-1 ↔ 7.0	+1 ↔ 9.0
D: Temperature, K	308.0	328.0	-1 ↔ 313.0	+1 ↔ 318.0

RESULTS AND DISCUSSION

Contact Time's Impact on Methylene Blue Adsorption

Figure-2a illustrates how the abundance of active sites causes methylene blue adsorption onto the prepared adsorbent to increase quickly in the first 20 minutes, followed by a slower phase until equilibrium is reached at about 30 minutes. Because of site saturation, higher initial dye concentrations result in a lower percentage removal, while lower concentrations increase uptake efficiency. This quick equilibrium achievement demonstrates the adsorbent's potential for effective dye removal from aqueous solution.

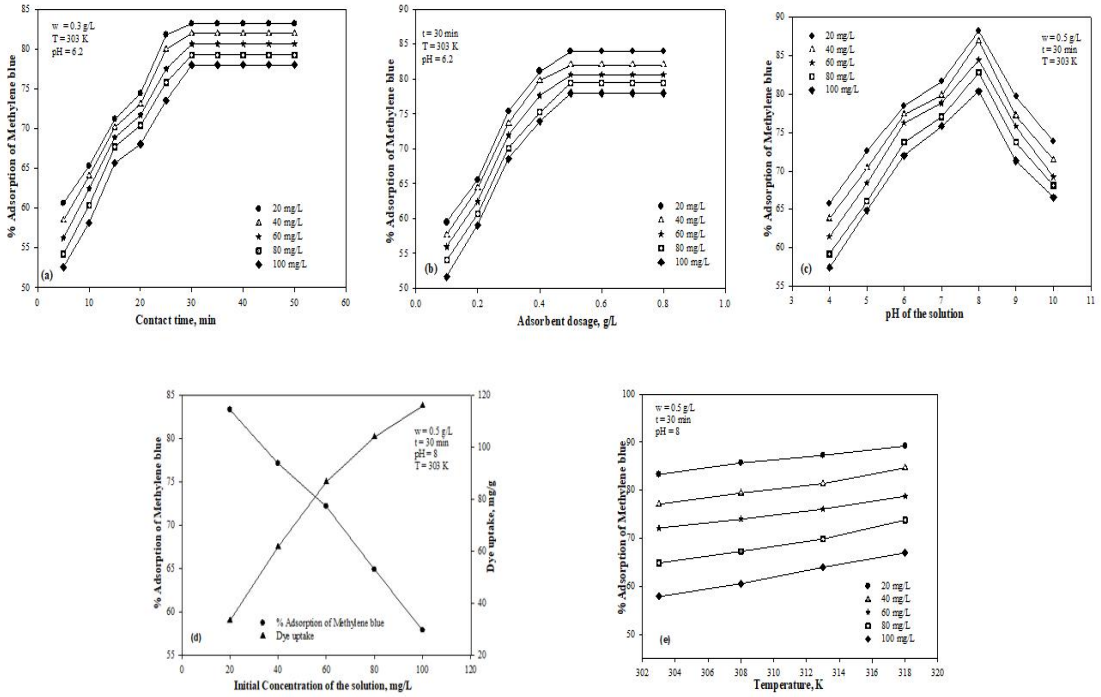

Fig.-2: (a) Contact Time's Impact on MB Adsorption at Different Starting Concentrations; (b) MB removal at Varying Initial Concentrations as a Function of Adsorbent Dosage; (c). The Role of Solution pH in MB Adsorption Onto Green-Synthesised CuNPs Was Assessed; (d) The Influence of Initial MB Concentration on CuNPs Adsorption; (e) Temperature's Impact on Green-Synthesised CuNPs' Adsorption of MB at Different Starting Concentrations.

Dosage of Nanoparticles Affects Methylene Blue Adsorption

Before plateauing, which indicates site saturation, the adsorption of methylene blue rose dramatically with adsorbent dosage up to 0.5 g/L (Fig.-2b). Higher removal efficiencies were observed at lower initial dye concentrations, which is indicative of less competition for the available active site. These findings validate the high affinity of green-synthesised CuNPs for MB and the necessity of dosage optimisation for economical treatment.

Influence of Solution pH on Adsorption Efficiency of Methylene Blue

The methylene blue adsorption onto CuNPs showed a clear pH dependence, rising gradually from pH 4 to a peak at pH 8, then declining at higher pH values, as shown in Fig.-2c. The better dye-surface interactions and less electrostatic repulsion are responsible for the enhanced removal around pH 8, whereas charge repulsion and competition with hydroxyl ions may be the cause of the decrease beyond this point. These findings support the notion that pH is a crucial factor influencing adsorption efficiency.

Initial Concentration's Effect on Adsorption Efficiency and Dye Uptake

Fig.-2d showed that while dye uptake per unit mass of adsorbent increased, methylene blue's adsorption efficiency decreased as the initial dye concentration increased. This suggests that active sites are saturated at higher concentrations. The need to optimise initial concentration for efficient adsorption performance is highlighted by this trend, which reflects increased competition among dye molecules for scarce binding sites.

Thermal Effects on Green-Synthesised CuNPs' Adsorption Performance

As the temperature rose, the methylene blue adsorption efficiency increased steadily, confirming the process's endothermic nature depicted in Fig.-2e. The better removal efficiency at all concentrations are resulted from the higher temperatures because they enhanced the mobility of dye molecules and expanded the number of available active sites. These findings demonstrate that the inherently spontaneous and thermodynamically favourable adsorption process shows effective and energetically feasible adsorbate uptake.

Kinetics and Adsorption Isotherms of MB onto Green-Synthesised CuNPs

MB adsorption onto green-synthesised Cu-NPs exhibited a slower diffusion-controlled equilibrium after a quick initial uptake. As illustrated in Fig.-3a–d, the kinetic evaluation indicates that the adsorption proceeds predominantly through a chemisorption-driven mechanism, with the pseudo-second-order (PSO) model yielding the most accurate fit to the experimental data ($R^2 > 0.99$). While Freundlich ($n > 1$) suggested favourable heterogeneous binding, isotherm studies showed Langmuir's superior fit ($R^2 \approx 0.9996$), indicating monolayer adsorption with high capacity ($q_{max} \approx 169.49$ mg/g) as shown in Tables-2 and 3. All of these findings point to CuNPs as extremely effective adsorbents for persistent dye removal.[14-15]

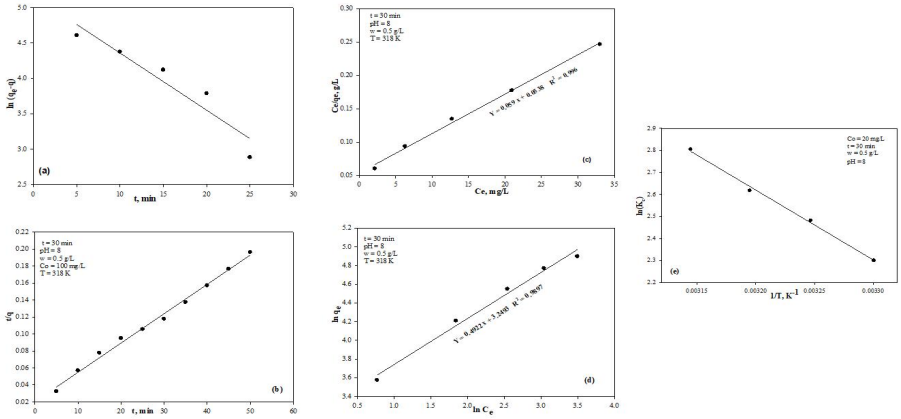

Fig.-3: (a and b). Kinetic Assessment of Green CuNPs in MB Adsorption Using PFO-PSO Models; (c and d). MB Adsorption Isotherms onto Green Synthesised CuNPs Fitted with Langmuir and Freundlich Models; (e). Plotting ln K_c against 1/T to Estimate Thermodynamic Variables for MB Adsorption onto Green-synthesised CuNPs.

Table-2: Kinetic Perspectives on MB Adsorption on Green Synthesised CuNPs.

Name of the kinetics	Parameter	Unit	Estimated value	R^2
Pseudo-first-order (PFO)	q_e	mg/g	174.862	0.9023
	k_1	1/min	0.0806	
Pseudo-second-order (PSO)	q_e	mg/g	285.715	0.9935
	k_2	g/mg. min	0.000606	

Table-3: Adsorption Isotherm Evaluation Parameters for MB Remediation onto Green Synthesised CuNPs.

Name of the isotherm	Parameter	Unit	Estimated value	R^2
Langmuir	q_{max}	mg/g	169.492	0.9996
	b	L/mg	0.10966	
Freundlich	K_f	$((mg/g)(L/mg)^{1/n})$	25.772	0.9877
	n	--	2.0316	

Green-Synthesised CuNPs for Adsorption of MB Thermodynamic Perspectives

The spontaneous and favourable nature of MB adsorption was confirmed by thermodynamic analysis, which showed negative ΔG° values, as presented in Fig. 3e and Table-4. The endothermic process, with adsorption enhanced at higher temperatures, was indicated by the positive ΔH°. A positive ΔS° value suggests enhanced disorder at the solid–liquid interface, likely arising from structural rearrangements on the adsorbent surface and the displacement of water molecules during the adsorption of the dye.

Table-4: Thermodynamic Parameter Summaries for Methylene Blue Adsorption onto Green Synthesized CuNPs.

T (K)	ln(k_c)	ΔG° (kJ/mol)	ΔH° (kJ/mol)	ΔS° (J/mol K)
303	2.300	-5.794	26.4468016	106.410886
308	2.482	-6.355		
313	2.617	-6.811		
318	2.805	-7.416		

Using Response Surface Methodology for Process Optimisation

Design-Expert (v8.0.7.1) was used to analyse thirty experimental runs shown in Table-5, and the results showed a high degree of agreement between the expected and actual responses observed in Fig.-4a. The high significance of the quadratic model was validated by ANOVA ($F = 31.72$, $p < 0.0001$, $R^2 = 0.9673$, Adeq Precision = 17.9428), tabulated in Table-6. With significant interactions between pH–dosage and temperature–concentration, pH and CuNPs dosage had the most significant effects. Robust optimisation within the design space is ensured by the validated quadratic model (Eq.-9), which effectively describes variables that impact MB removal efficiency.[8,13]

Percentage Adsorption of Methylene Blue = + 88.48 + 0.4746 A - 0.0663 B + 0.3471 C + 0.0796 D + 0.2231 AB - 0.1881 AC + 0.1181 AD - 0.0119 BC + 0.8369 BD - 0.3494 CD - 1.44 A^2 - 1.23 B^2 - 1.67 C^2 - 1.14 D^2 (9)

With ideal conditions (pH 8.1, dosage 0.49 g/L, concentration 20.5 mg/L, temperature 317.7 K), achieving 88.5% efficiency, the coded quadratic model (–1 to +1) successfully predicted MB removal, closely matching experimental validation results (Fig.-4b). In addition to reducing experimental runs, RSM also made parameter interactions more understandable and validated surface-controlled adsorption. The antagonistic and synergistic effects of variable pairs on MB removal were further demonstrated by three-dimensional response surfaces are shown in Fig.-4c-h.

Table-5: Experimental Matrix for Central Composite Design (CCD) for Improving Methylene Blue Elimination with CuNPs Derived from Litchi Seed extract.

Run No.	Initial MB Concentration mg/L	NPs dosage g/L	pH	Temperature K	Experimental Value	Predicted Value
1	15	0.4	7	323	81.02	81.74
2	25	0.4	7	313	83.11	83.44
3	25	0.6	7	323	84.72	84.87
4	20	0.5	8	318	88.48	88.48

5	20	0.5	8	318	88.48	88.48
6	15	0.6	9	323	83.34	83.21
7	20	0.5	10	318	82.17	82.48
8	15	0.6	9	313	82.33	82.31
9	15	0.6	7	323	83.76	82.86
10	20	0.5	8	308	83.98	83.75
11	15	0.4	9	323	82.06	82.14
12	15	0.4	9	313	84.54	84.59
13	20	0.5	8	318	88.48	88.48
14	15	0.4	7	313	83.42	82.80
15	30	0.5	8	318	83.12	83.69
16	20	0.3	8	318	83.65	83.71
17	10	0.5	8	318	82.08	81.79
18	15	0.6	7	313	79.45	80.57
19	20	0.5	6	318	81.12	81.09
20	25	0.6	9	313	83.62	83.10
21	25	0.4	7	323	83.32	82.86
22	20	0.7	8	318	83.23	83.45
23	25	0.4	9	313	84.06	84.48
24	20	0.5	8	318	88.48	88.48
25	25	0.6	9	323	84.32	84.47
26	20	0.5	8	328	83.55	84.06
27	20	0.5	8	318	88.48	88.48
28	20	0.5	8	318	88.48	88.48
29	25	0.4	9	323	83.42	82.50
30	25	0.6	7	313	82.66	82.10

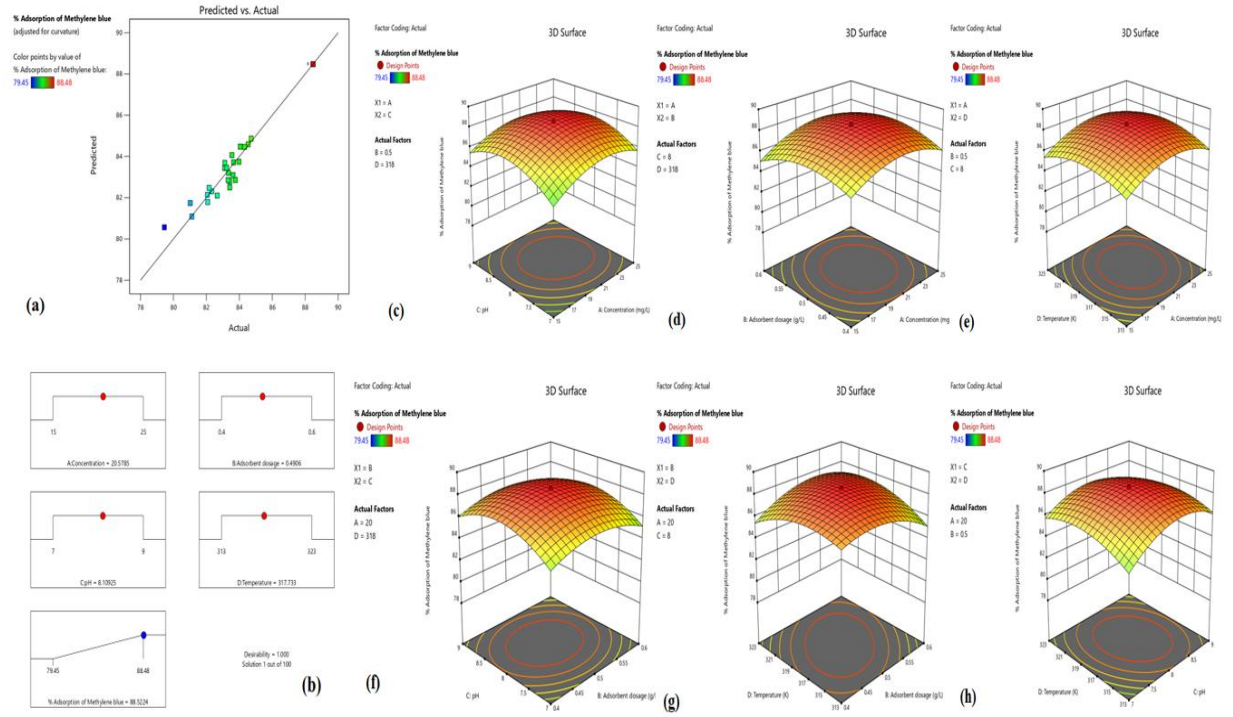

Fig.-4: (a) Litchi Seed-Derived CuNPs' Predicted and Experimental MB Removal Efficiencies; (b) Desirability Ramp Plot for Optimal MB Elimination with CuNPs Derived from Litchi Seeds; (c-h) 3D Response Surface Plots Showing How Process Variables Interact to Affect the Effectiveness of MB Removal.

Table-6: ANOVA Overview of the Response Surface Quadratic Model for Maximising the Removal of Methylene Blue using CuNPs Derived from Litchi Seeds Extract

Source of Variation	Sum of Squares (SS)	Degrees of freedom (df)	Mean Square (MS)	F-value	p-value
Model	172.74	14	12.34	31.72	< 0.0001
A- Initial dye Concentration, mg/L	5.41	1	5.41	13.90	0.0020
B-Adsorbent dosage, g/L	0.1053	1	0.1053	0.2708	0.6104
C- Solution pH	2.89	1	2.89	7.43	0.0156
D-Temperature, K	0.1520	1	0.1520	0.3908	0.5413
AB	0.7966	1	0.7966	2.05	0.1729
AC	0.5663	1	0.5663	1.46	0.2463
AD	0.2233	1	0.2233	0.5740	0.4604
BC	0.0023	1	0.0023	0.0058	0.9403
BD	11.21	1	11.21	28.81	< 0.0001
CD	1.95	1	1.95	5.02	0.0406
A^2	56.49	1	56.49	145.23	< 0.0001
B^2	41.17	1	41.17	105.83	< 0.0001
C^2	76.85	1	76.85	197.57	< 0.0001
D^2	35.89	1	35.89	92.26	< 0.0001
Residual Error	5.83	15	0.3890		
Lack of Fit	5.83	10	0.5835		
Pure Error	0.0000	5	0.0000		
Corrected Total	178.57	29			
Adjusted R^2	0.9368				
Predicted R^2	0.8118				
Adeq Precision	17.9428				

CONCLUSION

The green-synthesised CuNPs exhibited pseudo-second-order kinetics, high-capacity Langmuir monolayer chemisorption, and rapid uptake (169.49 mg/g), demonstrating strong potential as efficient and sustainable adsorbents for methylene blue. Their stability, strong dye affinity, and eco-friendly synthesis support their suitability for large-scale wastewater treatment, in line with SDG 6.

ACKNOWLEDGMENTS

The authors express their sincere gratitude to their professors for their invaluable advice and assistance.

CONFLICT OF INTERESTS

The authors declare that there is no conflict of interest.

AUTHOR CONTRIBUTIONS

The present work is related to *SDG-6: Clean Water and Sanitation*. All the authors contributed significantly to this manuscript, participated in reviewing/editing and approved the final draft for publication. The research profile of the authors can be verified from their ORCID ids, given below:

Pampana Anil Kumar https://orcid.org/0009-008-6780-5889
J. A. Suhasini https://orcid.org/0000-0002-5399-2635
M. Sudheera https://orcid.org/0000-0001-8012-7527
Pulipati King https://orcid.org/0000-001-8210-3019
D. Appala Naidu https://orcid.org/0000-0002-2355-4394
Meena Vangalapti https://orcid.org/0000-0002-7303-8160

Cite this article as: P. K. Kumar *et al.*, *Rasayan J. Chem.*, 19(1), 483-491(2026), https://doi.org/10.31788/RJC.2026.1919585.

REFERENCES

1. M. Eltaweil, M. E. Elshazly and H. Abd El-Monaem, *Journal of Environmental Chemical Engineering*, **11**, 20 (2023).
2. N. Gomaa, A. Z. Elsherbiny and S. Ibrahim, *Environmental Science and Pollution Research*, **29**, 50914(2022).
3. H. T. Aljuboury, S. Palaniandy and A. F. Abdul Wahab, *Environmental Technology and Innovation*, **25**, (2022).
4. A. S. Naseem, M. Hameed and F. Ahmad, *Advances in Natural Sciences: Nanoscience and Nanotechnology*, **15**, (2024).
5. D. N. Shetty, V. A. Lobo, S. Rani and N. R., *Hybrid Advances*, **7**, 100316(2024), https://doi.org/10.1016/j.hybadv.2024.100316.
6. W. K. Essa, *Chemistry*, **6**, 249(2024), https://doi.org/10.3390/chemistry6010012.
7. S. Moral, J. R. García and M. T. San Miguel, *ACS Omega*, **7**, 26590(2024).
8. C. A. Igwegbe, L. Mohmmadi, S. Ahmadi, A. Rahdar, D. Khadkhodaiy, R. Dehghani and S. Rahdar, *MethodsX*, **6**, 1779(2019), https://doi.org/10.1016/j.mex.2019.07.016.
9. A. Gupta and C. Balomajumder, *Applied Water Science*, **7**, 4361–4364 (2017).
10. B. Farasati Far, M. R. Naimi-Jamal, M. Jahanbakhshi *et al.*, *Scientific Reports*, **14**, 19217(2024), https://doi.org/10.1038/s41598-024-69969-1.
11. Y. Miyah, A. Lahrichi, M. Idrissi, A. Khalil and F. Zerrouq, *Surfaces and Interfaces*, **11**, 74(2018), https://doi.org/10.1016/j.surfin.2018.03.006.
12. I. S. Aldabagh, D. N. Saad and E. I. Ahmed, *Chemical Engineering Journal Advances*, **18**, 100608(2024), https://doi.org/10.1016/j.ceja.2024.100608.
13. S. Soudagar, S. Akash, M. S. Venkat, V. R. Poiba and M. Vangalapati, *Materials Today: Proceedings*, **59**, 667(2022), https://doi.org/10.1016/j.matpr.2021.12.199.
14. V. R. Poiba, B. Sowjanya, P. King and M. Vangalapati, *Advances in Materials and Processing Technologies*, **10**, 3013(2023), https://doi.org/10.1080/2374068X.2023.2192393.
15. S. Sahu, S. Pahi, S. Tripathy, S. K. Singh, A. Behera, U. K. Sahu and R. K. Patel, *Journal of Molecular Liquids*, **315**, 113743(2020), https://doi.org/10.1016/j.molliq.2020.113743.

[RJC-9585/2025]